# Valence Bond Approach of Metal–Ligand Bonding in the Dewar–Chatt–Duncanson Model

**ARTICLE** *in* INORGANIC CHEMISTRY · JANUARY 2008

Impact Factor: 4.76 · DOI: 10.1021/ic701434e · Source: PubMed



**3 AUTHORS:**

Mathieu Linares
Linköping University
**63** PUBLICATIONS **982** CITATIONS
SEE PROFILE

Benoît Braïda
Pierre and Marie Curie University - Paris 6
**47** PUBLICATIONS **695** CITATIONS
SEE PROFILE

Stéphane Humbel
Aix-Marseille Université
**62** PUBLICATIONS **2,823** CITATIONS
SEE PROFILE

*Inorg. Chem.* **2007**, *46*, 11390–11396


# Valence Bond Approach of Metal–Ligand Bonding in the Dewar–Chatt–Duncanson Model

**Mathieu Linares,[†] Benoit Braida,*[,‡] and Stéphane Humbel*[,†]**

*UMR 6180 - Chirotechnologies: Catalyse et Biocatalyse, CNRS/Université Paul Cézanne (Aix-Marseille III), Campus St Jérôme Case A 62, 13397 Marseille Cedex 20, France, Laboratoire de Chimie Théorique − UMR 7616 CNRS/Université Pierre et Marie Curie, "Le Raphaël", 3 rue Galilée, 94200 Ivry-Sur-Seine CEDEX, France*

Received July 20, 2007

Metal–ligand bonding, as considered in the Dewar–Chatt–Duncanson model, is described via an ab initio Valence Bond (VB) approach and applied to typical Pd–L complexes (L = $NH_3$, $PH_3$, $CH_2$, $SiH_2$). A progressive construction of the VB wave function is followed and leads to a very compact, though accurate, description of metal–ligand bonds. A description with the donation interaction only (ligand–metal) is first constructed and enriched so the back-donation interactions (metal–ligand) are also introduced. This latter VB wave function, although being extremely compact, provides bonding energies in agreement with standard (correlated) methods. A comparison between the two VB levels allows a quantification of adiabatic back-bonding energies and reveals very different trends between the ligands considered. A very faint back-donation in Pd–$NH_3$ is found, which contrasts with a significant effect in Pd–$PH_3$. Back-donation is, however, more important in Pd–$XH_2$ complexes. In Pd–$CH_2$, it is such that it even represents the major source of bonding. For Pd–$SiH_2$, back-donation is slightly weaker than donation. The nature of the interaction in these metal–ligand complexes is revealed by the VB wave function analysis. Results are as well rationalized using the simple molecular orbital picture and compared to previous studies.

## Introduction

Metal−ligand bonding in transition-metal complexes is commonly separated into donation ($\sigma$ bond) and back-donation ($\pi$ bond) components through the Dewar−Chatt−Duncanson's (DCD) derived model.[1,2] This model, depicted in Scheme 1, has been fruitfully used in many transition-metal studies.[3] Following this model, methods for quantifying $\sigma$ and $\pi$ components in a metal−ligand interaction have been designed in several previous studies and have given insights into metal−ligand bondings.[4−7] Bagus and Pacchioni used the constrained space orbital variation method (CSOV) to provide some estimates of donation versus back-donation effects.[5] They have particularly shown on Pd−$PX_3$ complexes (where X = H, $CH_3$, $OCH_3$, F) that d orbitals are an

**Scheme 1**

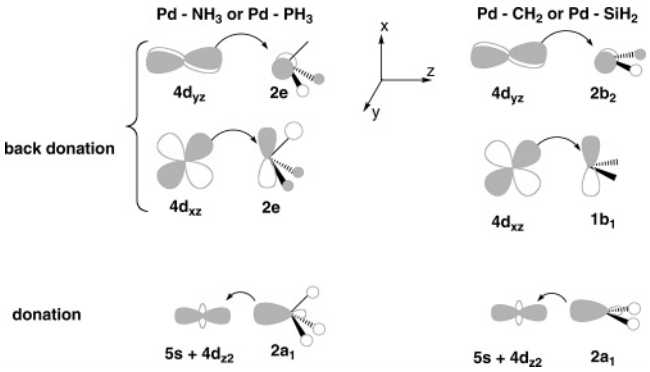


* To whom correspondence should be addressed. E-mail: braida@lct.jussieu.fr (B.B.), stephane.humbel@univ-cezanne.fr (S.H.).
[†] CNRS/Université Paul Cézanne (Aix-Marseille III).
[‡] CNRS/Université Pierre et Marie Curie.

(1) Dewar, M. J. S. *Bull. Soc. Chem. Fr.* **1951**, *18*, C71.
(2) Chatt, J.; Duncanson, L. A. *J. Chem. Soc.* **1953**, 2939.
(3) See, for instance, these reviews and references therein: Frenking, G.; Fröhlich, N. *Chem. Rev.* **2000**, 100, 717. Dedieu, A. *Chem. Rev.* **2000**, 100, 543; Hargittai, M. *Chem. Rev.* **2000**, *100*, 2233.
(4) For a recent examination of the DCD model with modern quantum chemical methods, see, for instance, Frenking, G. *J. Organomet. Chem.* **2001**, *635*, 9.
(5) Pacchioni, G.; Bagus. P. S. *Inorg. Chem.* **1992**, *31*, 4391.
(6) (a) Bagus, P. S.; Hermann, K.; Bauschlicher, C. W. *J. Chem. Phys.* **1984**, *80*, 4378. (b) Bagus, P. S.; Hermann, K.; Bauschlicher, C. W. *J. Chem. Phys.* **1984**, *81*, 1966. (c) Bagus, P. S.; Hermann, K.; Bauschlicher, C. W. *J. Chem. Phys.* **1984**, *81*, 5890. (d) Bauschlicher, C. W.; Bagus, P. S.; Nelin, C. J.; Roos, B. 0. *J. Chem. Phys.* **1986**, *85*, 354.
(7) Ziegler, T.; Rauk, A. *Theor. Chim. Acta* **1977**, *46*, 1.



10.1021/ic701434e CCC: $37.00 
Published on Web 11/29/2007

important ingredient for back-donation. More than a third of the back-donation energy is indeed lost when d orbitals on the phosphorus atom are not used. Beside the role of the d orbitals, Bagus and Pacchioni's analysis provides indicative values for donation energies (around 10 kcal/mol in the Pd−$P(CH_3)_3$ complex for instance). It is also found that back-donation increases in the series $P(CH_3)_3 < PH_3 < P(OCH_3)_3 < PF_3$, which is consistent with the lowering of the anti bonding 2e orbitals by electron $\sigma$-attractive substituents. However, this approach relies on an uncorrelated wave function,[8] whereas electronic correlation is crucial in a metal−ligand bond. Separating bonding and back-bonding components can be achieved as well through an energy decomposition analysis method, like the extended transition state method by Ziegler and Rauk.[7,9] This approach gives a breakdown of the bonding energy into steric and electronic terms, the latter being further separated into $\sigma$ and $\pi$ bond related terms. In more recent studies, this type of analysis has been extended to understanding the bonding in transition states.[10] Clear and elegant differentiation of the back-bonding effects was found, for instance in chromium−carbene or chromium−silenes systems,[11] and even more recently in ruthenium−(C) and iron−(C) for instance.[12]

Through the DCD picture, the metal−ligand interaction is hence considered to arise from the energetic stabilization as a result of electron pairs delocalization, from ligand to metal (donation) on the one hand, and from metal to ligand (back-donation) on the other hand. As it relies on localized electrons and orbitals, valence bond (VB)-based approaches should be particularly suited to devise a quantum chemical description of metal−ligand bonds based on this picture.

Accurate dissociation energies were not obtained in preliminary VB approaches because they missed the dynamical correlation energy, which usually requires a large and complicated wave function. In recent VB approaches,[13] this important part of the correlation has been efficiently included by allowing the instantaneous adaptation (the breathing) of the orbitals to the charge fluctuation that occurs in the bond. Such a breathing orbital effect (BO effect) is taken into account when using different orbitals for different VB structures. As depicted in the upper part of Scheme 2 for the donation only, the orbitals of the ligand, for instance, are more diffuse if the two bonding electrons are located on

**Scheme 2**

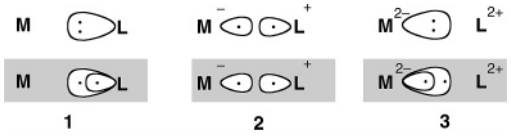


the ligand as in **1**, and they are more compact when one bonding electron is located on the ligand, as in **2**. The same principle holds for all of the orbitals of the system. Even more accurate descriptions of bond dissociation energies were obtained using mono-occupied orbitals as shown in the lower part of the scheme. Although this approach is computationally demanding, it allows keeping a compact and readable wave function all along the dissociation path (vide infra), whereas it has been proven to give accurate dissociation curves and bonding energies for small organic molecules and metal-hydride cations.[13b,14] We use here a specific definition of the VB wave function, partly based on the BO concept, designed to reach an accurate as well as readable description of metal−ligand bonding.[15]

For the metal−ligand bond-breaking processes we are describing here, the donation interaction is first described in our VB wave function through the traditional three VB structures expansion (one covalent plus two ionics), using mono-occupied orbitals and including the BO effect. In a second stage, back-donation is introduced by simply letting the metal−$\pi$ electron pairs to delocalize onto the appropriate ligand's orbitals (vide infra). As we will see, this latter VB wave function includes the most relevant part of the correlation energy, and it will allow us to rigorously separate and accurately quantify the respective donation and back-donation contributions to the bonding.

We have chosen to apply our VB approach to Pd−L complexes because palladium gives rise to transition-metal complexes of great chemical interest. Besides, as an electron rich metal, it is likely to significantly back-donate some of its electron pairs to the ligand. We considered four typical ligands: $NH_3$, $PH_3$, $CH_2$, $SiH_2$, which model a broad range of situations. On the one hand, this choice allows a comparison of the back-donation to an anti bonding ligand orbital (amine and phosphine), versus back-donation to a nonbonding p vacant orbital (singlet carbene and silene). On the other hand, it enables a comparison between a second-row (amine and carbene) and a third-row (phosphine and silene) metal−ligand bond.

## Computational Details

In this study we used the lanl2dz[16] electron core potential (ECP) for all of the heavy atoms. As suggested in the literature,[5] polarization (d) orbitals are added to the basis set that comes with the lanl2dz ECP for nonmetallic heavy atoms. The coefficients for

(8) Inclusion of correlation energy in the CSOV approach has been only recently achieved via DFT related computations: Piquemal, J. P.; Marquez, A.; Parisel, O.; Giessner-Prettre, C. *J. Comp. Chem.* **2005**, *26*, 1052.

(9) For a recent use of such an approach see, for instance, Bessac, F.; Frenking, G. *Inorg. Chem.* **2006**, *45*, 6956.

(10) (a) Bickelhaupt, F. M. *J. Comp. Chem.* **1999**, *20*, 114. (b) An interesting review on the use of DFT that includes this fragment decomposition analysis can be found in Bickelhaupt, F. M.; Baerends, E. J. *Reviews in Computational Chemistry*; K. B. Lipkowitz, D. B. Boyd, Eds.; Wiley-VCH: New York, 2000; Vol. 15, pp 1−86.

(11) (a) Jacobsen, H.; Ziegler, T. *Organometallics* **1995**, *14*, 224. (b) *Inorg. Chem.* **1996**, *35*, 775.

(12) Krapp, A; Pandey, K. K.; Frenking, G. *J. Am. Chem. Soc.* **2007**, *129*, 7596.

(13) (a) Hiberty, P. C.; Flament, J. P.; Noizet, E. *Chem. Phys. Lett.* **1992**, *189*, 259. (b) Hiberty, P. C.; Humbel, S.; Archirel, P. *J. Phys. Chem.* **1994**, *98*, 11697. (c) Hiberty, P. C.; Humbel, S.; Byrman, C. P.; Vanlenthe, J. H. *J. Chem. Phys.* **1994**, *101*, 5969. (d) Hiberty, P. C.; Shaik, S. *Theor. Chem. Acc.* **2002**, *108*, 255.

(14) (a) Marynick, D. S. *J. Am. Chem. Soc.* **1984**, *106*, 4064. (b) Chen, E-H.; Chang, T-C. *J. Mol. Struct. (Theochem.)* **1998**, *431*, 127. (c) Gilheany, D. G. *Chem. Rev.* **1994**, *94*, 1339. (d) Orpen, A. G.; Connelly, N. *Organometallics* **1990**, *9*, 1206.

(15) Shurki, A; Hiberty, P. C.; Shaik, S. *J. Am. Chem. Soc.* **1999**, *121*, 822.

(16) (a) Hay, P. J.; Wadt, W. R. *J. Chem. Phys.* **1985**, *82*, 270. (b) Hay, P. J.; Martin, R. L. *J. Am. Chem. Soc.* **1992**, *114*, 2736.

these orbitals are taken from the D95(d) basis set and are equal to 0.80, 0.37, 0.75, and 0.32 for nitrogen, phosphorus, carbon, and silicium respectively. This basis set, together with the ECP, is referred to as lanl2dz* basis set. The B3LYP/lanl2dz* level is used to freely optimize the geometries of each complex using the *Gaussian 98* package.[17] This moderate-size basis set is used to construct dissociation curves at different levels of computations to show the main trends. However, for accurate predictions, a larger basis set is used to compute dissociation energies and equilibrium metal−ligand distances. For these extended-basis-set calculations, we used the Stuttgart relativistic small core pseudo potential together with the recommended basis set for palladium,[18] adding two polarization f functions from Martin and Sundermann.[19] The outer electrons of the palladium atom are thus described by a 6s5p3d2f contracted basis set. The ligands are described with unmodified cc-pvtz that corresponds to a 4s3p2d1f contraction for nitrogen and carbon atoms, for instance, and the cc-pvqz to a 5s4p3d2f1g contraction for the same atoms.[20]

We are aiming here at a partition of the dissociation energy with a clean VB methodology. The dissociation curves are constructed in the following way. A Pd−ligand distance is held fixed, and all of the other internal coordinates are relaxed at the B3LYP/lanl2dz* level. For each distance, the optimized geometry is subsequently used for VB and CCSD(T) single point calculations. Because no analytical gradients are available for our VB wave functions, we have used a simple quadratic approximation to establish the equilibrium distances and the bonding energies associated with the TZ VB computations. The VB-related calculations are carried out using the XMVB program from Wu and co-workers,[21] a modern and efficient spin-free VB code. It allows a full flexibility for the definition of any VB-related wave function, including VBSCF, BOVB,[13] VBB,[22] or VBCI method.[21c] For VB computations using the TZ basis set, we encountered convergence difficulties in third-row ligands ($PH_3$ and $SiH_2$). These difficulties were related to the fact that the orbitals could escape from their local characteristics in using the most-diffuse functions of the TZ basis set. This pushed us to a partial-VB optimization of some of the orbitals of the $PdPH_3$ and $PdSiH_2$ system (vide infra).

**Definition of the Valence-Bond Wave Function for Metal−Ligand Bonding.** We differentiate active and inactive sets of electrons in our wave functions. The six electrons directly involved in the bonding, either for donation (two of them) or for back-donation interaction (four of them) are called active, and all of the other electrons are called inactive. Most of the inactive electrons occupy metal (1s, 2s 2p, 3s, 3p, 3d) or fragment heavy-atom core orbitals (1s, 2s, and 2p for phosphorus and silicon). These electrons are described through the pseudo potential, which means that they are not explicitly considered. The remaining inactive electrons, with the exception of the 5s, are explicitly considered in the wave function as doubly occupied orbitals centered at each fragment. The description of six active electrons led to two different VB wave functions, the first one with donation only and the second one including back-donation interaction as well.

**The VB Wave Function with Donation Only.** The $\sigma$ bond (donation) comes from the delocalization of the ligand $2a_1$ lone pair to a mixing of 5s, $4p_z$, and $4d_{z^2}$ orbitals on the metal (Scheme 1). It can thus be described through the traditional covalent/ionic VB expansion for a two-electron pair bond, by the three VB structures depicted in Scheme 2. These structures are built using non-orthogonal orbitals that are either a combination of strictly localized metal-atomic orbitals (s, $p_z$ and $d_{z^2}$) or fragment molecular orbitals (MOs) localized on the ligand moiety. The four other active electrons occupy $d_{xz}$ and $d_{yz}$ orbitals strictly localized on the metal, thus preventing any back-bonding interaction to take place through delocalization onto the ligand. The 5s electron pair is described by a couple of mono-occupied orbitals in the lanl2dz* basis-set computations and by a doubly occupied orbital for the TZ basis-set computations. Thus, for each of the three active pairs, the two electrons occupy two different singlet-coupled mono-occupied local orbitals, whether it is a covalent pair (one electron located on each center), or a lone/ionic pair (the two electrons on the same center). The breathing orbital (BO) effect is fully introduced here, each structure having its specific set of active and inactive orbitals. All of the orbitals and structure coefficients are optimized simultaneously, following the variational principle and the localization constraints, leading to our VB−I level of computation. The orbitals can particularly repolarize themselves and adapt in shape (diffuseness) to the charge fluctuation, when going from covalent to ionic situations.

**Introduction of the Back-Donation into the VB Wave Function.** The $\pi$ palladium−ligand bond originates from the stabilization induced by the delocalization of the two metal 4d electron pairs onto the ligand's empty orbital of compatible symmetry (Scheme 1). Describing the two $\pi$ interactions, as well as the $\sigma$ bond, using the three structure expansion for each (ionic and covalent) would require a total of 27 VB structures ($3 \times 3 \times 3$). Such a number is not beyond the reach of current computers, but the computational cost would be high because of the use of different orbital sets for each structure (BO effect). More importantly, such a wave function would be too complicated for a straightforward analysis. Hence, to keep a more compact wave function, back-donation is introduced by simply letting the metal-active $\pi$ lone pairs freely delocalize on the neighboring ligand orbitals of compatible symmetry. This can be done without increasing the size of the wave function, by using for each $\pi$ bond a pair of Coulson−Fisher type of non-orthogonal

(17) Frisch, M. J.; Trucks, G. W.; Schlegel, H. B.; Scuseria, G. E.; Robb, M. A.; Cheeseman, J. R.; Zakrzewski, V. G.; Montgomery, J. A., Jr.; Stratmann, R. E.; Burant, J. C.; Dapprich, S.; Millam, J. M.; Daniels, A. D.; Kudin, K. N.; Strain, M. C.; Farkas, O.; Tomasi, J.; Barone, V.; Cossi, M.; Cammi, R.; Mennucci, B.; Pomelli, C.; Adamo, C.; Clifford, S.; Ochterski, J.; Petersson, G. A.; Ayala, P. Y.; Cui, Q.; Morokuma, K.; Malick, D. K.; Rabuck, A. D.; Raghavachari, K.; Foresman, J. B.; Cioslowski, J.; Ortiz, J. V.; Stefanov, B. B.; Liu, G.; Liashenko, A.; Piskorz, P.; Komaromi, I.; Gomperts, R.; Martin, R. L.; Fox, D. J.; Keith, T.; Al-Laham, M. A.; Peng, C. Y.; Nanayakkara, A.; Gonzalez, C.; Challacombe, M.; Gill, P. M. W.; Johnson, B. G.; Chen, W.; Wong, M. W.; Andres, J. L.; Head-Gordon, M.; Replogle, E. S.; Pople, J. A. *Gaussian 98*, revision A.11; Gaussian, Inc.: Pittsburgh, PA, 1998.

(18) (a) Basis sets, including the pseudopotential definition were obtained from the Extensible Computational Chemistry Environment Basis Set Database, Version 02/02/06, as developed and distributed by the Molecular Science Computing Facility, Environmental and Molecular Sciences Laboratory, which is part of the Pacific Northwest Laboratory, P.O. Box 999, Richland, Washington 99352, U.S.A., and funded by the U.S. Department of Energy. http://www.emsl.pnl.gov/forms/basisform.html (b) Bergner, A.; Dolg, M.; Kuechle, W.; Stoll, H.; Preuss, H. *Mol. Phys.* **1993**, *80*, 1431. (c) Kaupp, M.; Schleyer, P. v. R.; Stoll, H.; Preuss, H. *J. Chem. Phys.* **1991**, *94*, 1360. (d) Dolg, M.; Wedig, U.; Stoll, H.; Preuss, H. *J. Chem. Phys.* **1987**, *86*, 866. (e) Dolg, M.; Stoll, H.; Preuss, H. Pitzer, R. M. *J. Phys. Chem.* **1993**, *97*, 5852.

(19) The recommended values for the exponents of the f functions in Pd are 0.621 and 2.203, see Martin, J. M. L.; Sundermann, A. *J. Chem. Phys.* **2001**, *114*, 3408.

(20) (a) Dunning, T. H. Jr. *J. Chem. Phys.* **1989**, *90*, 1007. Woon D. E.; Dunning, T. H.; Jr. *J. Chem. Phys.* **1993**, *90*, 1358.

(21) (a) Song, L.; Wu, W.; Mo, Y.; Zhang, Q. XMVB-01: An ab initio Nonorthogonal Valence Bond Program, Xiamen University, Xiamen 361005, China, 2003. (b) Song, L. C.; Mo, Y. R.; Zhang, Q. N.; Wu, W. *J. Comput. Chem.* **2005**, *26*, 514. (c) Wu, W.; Song, L. C.; Cao, Z. X.; Zhang, Q.; Shaik, S. *J. Phys. Chem. A* **2002**, *106*, 2721.

(22) Linares, M.; Braida, B.; Humbel, S. *J. Phys. Chem. A* **2006**, *110*, 2505.

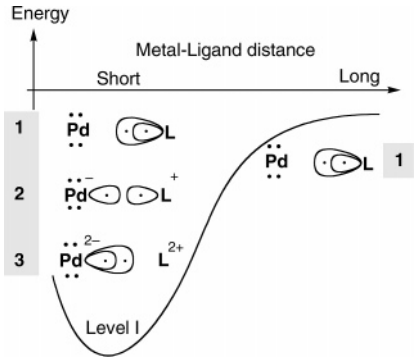


**Figure 1.** Dissociation curve with the $\sigma$ donation included. Dissociation to the neutral fragments M + L.

**Scheme 3**

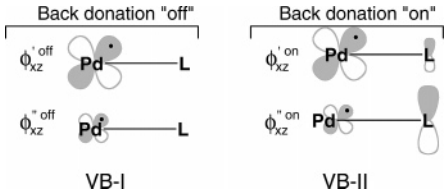


orbitals, ($\phi'$, $\phi''$), in the spirit of the GVB wave function.[23] Switching on the $\pi$ interaction by allowing this delocalization is depicted for the $d_{xz}$ case in Scheme 3 above. The paired electrons still occupy two different spin orbitals, mainly localized on the metal, but when the delocalization to the ligand is allowed, these orbitals develop a small component on the ligand basis functions of compatible symmetry. Singlet-coupling the two electrons in two different delocalized non-orthogonal orbitals implies an indirect introduction of covalent/ionic mixing through orbital optimization.[23b] Back-donation can thus be switched on at will, but the wave function is kept compact and readable, with only the three interacting structures. All of the other electron pairs ($\sigma$ bond, inactive electrons) are described in the same way as that in the VB−I level. Different sets of orbitals are used for different structures, enabling the BO effect to be accounted for. Such a description of the $\pi$ system is very similar to what is done through the Valence Bond BOND (Breathing Orbital Naturally Delocalized) (VBB) method we recently proposed.[22] In particular, this approach has been used to quantify $\pi$ substituent effects in carbonyl and haloallyl cations in a very similar way.[24]

As donation and back-donation strongly depend on the distance between metal and ligand, it is appealing to compute the dissociation curves for the Pd−L complexes mentioned above. With our VB wave function, the dissociation to the fragments M + L is treated in a balanced way compared to the associated complex (metal−ligand). As pictured in Figure 1, structures **2** and **3** would spontaneously and progressively vanish when the interatomic distance is increased; only **1** remains at the dissociation limit. Because the $\pi$ orbitals are treated using Coulson−Fischer (GVB) pairs at the VB−II level, their delocalization onto the neighboring ligand diminishes when the bond is stretched, ensuring a correct dissociation of $\pi$ bonds when back-bonding is included. The delocalization to the ligand's orbitals thus cancels at infinite an distance, which gives strictly localized orbital pairs, just as in the VB−I level. As a result, the two levels converge to the same wave function at the dissociation limit.

(23) (a) Coulson, C. A.; Fischer, I. *Philos. Mag.*, **1949**, *40*, 386. (b) Hiberty, P. C. *J. Mol. Struct. (Theochem.)* **1998**, *451*, 237.
(24) Linares, M.; Humbel, S.; Braida, B. *Faraday Discuss.* **2007**, *135*, 273.

## Results and Discussion

**The Metal−Ligand Bonding in Pd−$NH_3$, Pd−$PH_3$, Pd−$CH_2$, and Pd−$SiH_2$.** Dissociation curves for Pd−$XH_3$ and Pd−$XH_2$ complexes, at the VB−I (with donation) and VB−II levels (with back-donation additionally included) are shown in Figure 2 (lanl2dz* basis set), along with the CCSD-(T) curves. The CCSD(T) curves are shifted so that dissociated fragments share the same zero energy.

These complete dissociation curves allow us to obtain and to show up the main trends concerning these four systems, at a low computational cost. However, because basis-set dependency can be an important source of error here,[25] equilibrium distances and dissociation energies are computed as well, using the larger TZ basis set. Comparison between both basis sets are displayed in Table 1 below, for B3LYP and CCSD(T) reference calculations. B3LYP is reputedly basis-set independent,[26] but the accuracy of the CCSD(T) level usually strongly benefits from extending the basis set to Triple Zeta quality (vide infra). As mentioned in the literature, DFT methods might overestimate the bonding energies, as compared with CCSD(T).[27] However, the computations using the TZ basis set show a much better consistency between the B3LYP and the CCSD(T) bonding energies, with a 3−4 kcal/mol margin of error for all of the cases but Pd−$CH_2$ (7 kcal/mol). The equilibrium distances are also in better agreement.

The equilibrium distances and the bonding energies associated with the different levels of computation, for the TZ basis-set level, are displayed in Table 2 below. For the sake of comparisons, energies are shown along with Hartree−Fock (HF), B3LYP, and CCSD(T) predictions. For the HF computations, B3LYP geometries are used for the energies shown in Table 2.

Comparison between HF and coupled-cluster or B3LYP values in Table 2 highlights the importance of correlation in metal−ligand bonding. Half of the bonding energy is obtained at the HF level for the silene, only a third for Pd−$PH_3$ and Pd−$CH_2$, whereas no bonding is even predicted between palladium and $NH_3$.

Let us now consider the VB computations. The VB−I level gives the donation contribution to the total bonding energy. For M−$XH_3$ complexes, $\sigma$ bonds have a similar energy decomposition : 15 kcal/mol with the lanl2dz* basis set and only slightly more with the TZ basis set. For M−$XH_2$ complexes, the $\sigma$ bonding energy amounts to ∼30 kcal/mol. Such a result indicates that the orbitals $2a_1$ interact similarly with the empty orbital of the palladium atom. This interaction is usually driven by overlap and by energy considerations between the metal and ligand orbitals. A very simple way to assess the similar donation energy is to look at the ligands' $2a_1$ orbital energies (in atomic units), for instance at the

(25) We gratefully acknowledge here a pertinent referee remark on the subject.
(26) See, for instance, for dipole and quadrupole evaluation De Proft, F.; Tielens, F.; Geerlings, P *J. Mol. Struct. (Theochem.)* **2000**, *506*, 1.
(27) See, for instance, for overbinding in DFT methods (a) de Jong, G. T.; Geerke, D. P.; Diefenbach, A.; Bickelhaupt, F. M. *Chem. Phys.* **2005**, *313*, 261. (b) de Jong, G. T.; Bickelhaupt, F. M. *J. Phys. Chem. A* **2005**, *109*, 9685.

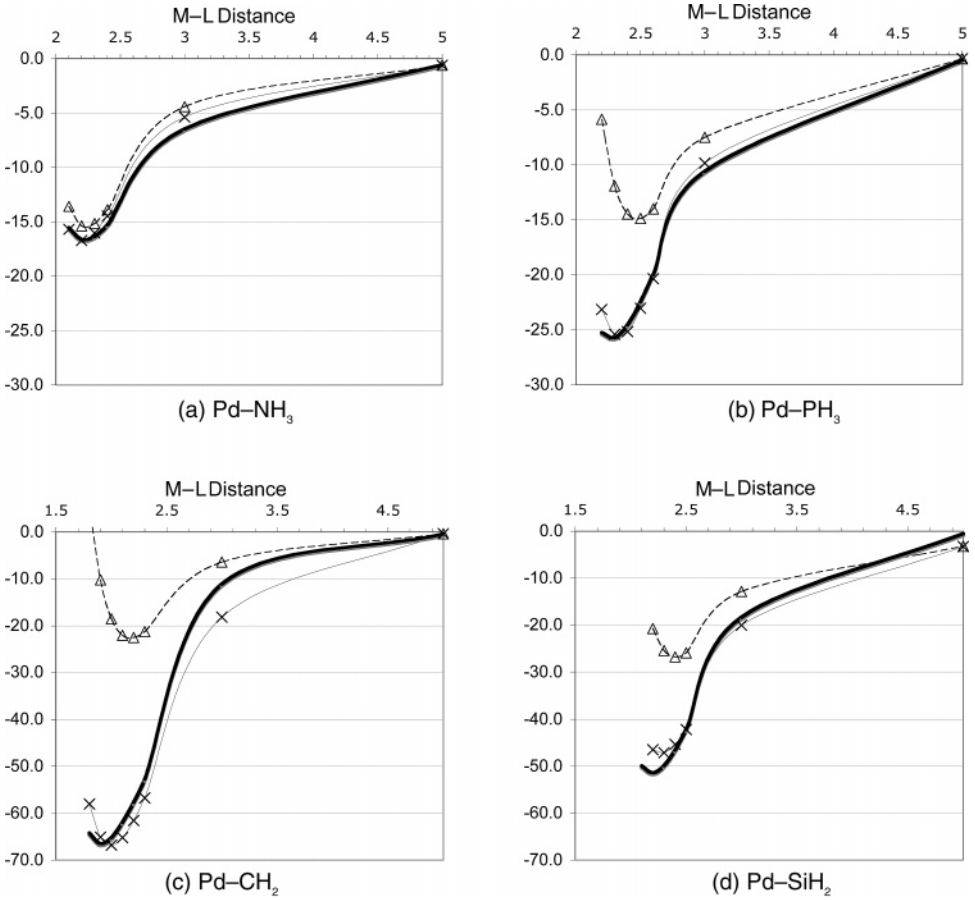


**Figure 2.** Calculations using the lanl2dz* basis set. Pd−$NH_3$, Pd−$PH_3$, Pd−$CH_2$, and Pd−$SiH_2$ dissociation curves for donation only (VB−I, △), donation plus back-donation (VB−II, ×), and at the CCSD(T) level (bold line). For Pd−$CH_2$ and Pd−$SiH_2$, the vertical scale is about twice as large as that for the other ligands, and the fragments are forced to dissociate to the lowest singlet states. Energies are in kcal/mol, distance in Å.

**Table 1.** BSSE Corrected Dissociation Energies (De in kcal/mol) and Equilibrium Distances (Re in Å) of the Metal−Ligand Complexes

| basis set | | level/ligand | $NH_3$ | $PH_3$ | $CH_2$ | $SiH_2$ |
|---|---|---|---|---|---|---|
| Lanl2dz* | De | B3LYP | 18.5 | 31.9 | 72.3 | 57.7 |
| | | CCSD(T) | 10.6 | 19.2 | 59.3 | 43.6 |
| | Re | B3LYP | 2.120 | 2.220 | 1.870 | 2.165 |
| | | CCSD(T) | 2.229 | 2.278 | 1.913 | 2.198 |
| TZ | De | B3LYP (TZ) | 19.8 | 37.0 | 75.2 | 59.9 |
| | | CCSD(T)(TZ) | 16.6 | 33.1 | 68.3 | 55.1 |
| | Re | B3LYP (TZ) | 2.100 | 2.176 | 1.846 | 2.148 |
| | | CCSD(T)(TZ) | 2.105 | 2.161 | 1.849 | 2.134 |

**Table 2.** Bond Dissociation Energies (kcal/mol) at the Different Valence Bond Levels and with Other Standard Ab Initio Methods for the Pd−$NH_3$, Pd−$PH_3$, Pd−$CH_2$, and Pd−$SiH_2$ Complexes

| | level | back-donation | Pd−$NH_3$ | Pd−$PH_3$ | Pd−$CH_2$ | Pd−$SiH_2$ |
|---|---|---|---|---|---|---|
| | HF[a] | | 2.4 | 12.5 | 26.5 | 27.6 |
| | CAS[a,b] | | 13.0 | 18.9 | 59.2 | 50.3 |
| | B3LYP (TZ)[c] | | 19.8 | 37.0 | 75.2 | 59.9 |
| TZ | CCSD(T)(TZ)[c] | | 16.6 | 33.1 | 68.3 | 55.1 |
| | VB−I (TZ) | off | 17.7 | 15.8 | 30.4 | 30.4 |
| | VB−II (TZ) | on | 19.0 | 26.9 | 69.2 | 52.5 |
| | *total back-donation (TZ)* | | *1.3* | *11.1* | *38.8* | *22.1* |

[a] B3LYP lanl2dz* optimized geometries are used. [b] CAS(12,12) for the complexes, CAS(10,10) for the palladium, CAS(2,2) for the ligand lone pair. [c] BSSE corrected values.

B3LYP/lanl2dz(*) level : $NH_3$, −0.2513; $PH_3$, −0.2690; $CH_2$, −0.2498; $SiH_2$, −0.2428. These values are close one to the other, which is consistent with the similar donation energies from these lone pairs. By going to the VB−II level, back-donation is switched on into the wave function. Except for the $PH_3$ ligand, where the agreement is moderate, the VB−II bonding energies differ by no more than 1−3 kcal/mol from the CCSD(T) predictions. This agreement is quite remarkable, considering the extreme compactness of the VB wave function we are using (only three structures) and the simple DCD model used. The agreement between the two approaches extends along to the whole dissociation curves (Figure 2, lanl2dz* basis set).

**Correlation Energy.** Compared to the CCSD(T) level, our VB−II wave function catches only a very small portion of the correlation energy. This can be shown on the dissociated fragments by comparing their *absolute* energies to those of the HF calculations. The absolute energies of these fragments at the VB−I level are only 14.2, 10.7, 13.1, and 10.6 kcal/mol lower than HF calculations for Pd + $NH_3$, Pd + $PH_3$, Pd + $CH_2$, and Pd + $SiH_2$, respectively. By contrast, the CCSD(T) total energies for Pd + $NH_3$ (for instance) are much lower than the HF energy, by about 180 kcal/mol, so that they account for a much-larger part of the correlation energy. However, a similar dissociation energy is obtained at the VB−II and CCSD(T) levels. We thus conclude that our approach catches the most-relevant parts of the correlation, the one that changes upon bonding. This catch of differential correlation is a characteristic of BOVB

**Table 3.** Triple ζ Basis Set Results at Selected Levels, Equilibrium Distances (Re in Å)

| level | Pd−$NH_3$ | Pd−$PH_3$ | Pd−$CH_2$ | Pd−$SiH_2$ |
|---|---|---|---|---|
| B3LYP | 2.100 | 2.176 | 1.846 | 2.148 |
| CCSD(T) | 2.105 | 2.161 | 1.849 | 2.134 |
| VB I | 2.336 | 2.495 | 2.117 | 2.372 |
| VB II | 2.323 | 2.283 | 1.985 | 2.200 |

methodologies and has been already encountered in small organic molecules as well as on metal-hydride cations.[13,15]

**Back-Donation Effects.** The comparison of the dissociation energies between VB−I and VB−II allows us to estimate the respective energetic effects of donation versus back-donation. As the geometries are optimized at each level of computation, adiabatic (nonvertical) delocalization energies are obtained,[28] although vertical energies could be found as well. Differences between the two levels show that, whereas back-donation is secondary in the Pd−$NH_3$ complex with about 1 kcal/mol of stabilization only, it is, on the contrary, significant in Pd−$PH_3$, where it amounts to about 11 kcal/mol, which is comparable to the $\sigma$ bond energy in these complexes (15 kcal/mol). This trend is not unexpected and is consistent with the molecular orbital (MO) picture. Indeed, whereas the $2a_1$ donating orbitals of the $NH_3$ and $PH_3$ ligands are close in energy, the 2e anti bonding orbitals (Scheme 1) of the $NH_3$ ligand are reputedly higher in energy than those of $PH_3$.[14] The latter being closer in energy to the couple of $4d_{xz}$ and $4d_{yz}$ degenerated orbitals, a larger back-donation is obviously obtained with phosphines than with amines.

For the Pd−$XH_2$ complexes and contrary to Pd−$XH_3$, the two back-donations in the *xz* and *yz* planes are not equivalent. The $1b_1$ orbital is indeed a low-lying nonbonding empty orbital that can easily accept the electrons from the $4d_{xz}$ orbital of the palladium to form a strong $\pi$ bond. On the contrary, the $2b_2$ orbital is an anti bonding orbital, and back-donation of the palladium $4d_{yz}$ orbital will be merest. We included here both effects at once. When back-donation is forbidden (VB−I), the interaction between palladium and carbene amounts to 30.4 kcal/mol. When the back-donation is included (VB−II), Pd−$CH_2$ bonding energy goes dramatically down to reach a total bonding energy of 69.2 kcal/mol, giving a bonding energy in correct agreement with coupled cluster and B3LYP. Hence, back-donation comes out to be the main source of bonding in palladium−carbene, with a total $\pi$ bonding of almost 40 kcal/mol. The energy associated with the back-donation in the silene is about twice as small as that in the carbene. This results are also consistent with Ziegler's analysis that, unlike carbenes, silenes exhibit a stronger $\sigma$ bond than a $\pi$ bond.[11]

**Geometrical Effect.** The optimized equilibrium distances obtained with the TZ basis set are displayed in Table 3. The bond distance predictions at the VB−II level are systematically larger than that with B3LYP or CCSD(T). This is a known behavior of VB methods including the BO effect.[13]

(28) Dewar, M. J. S.; Gleicher, G. J. *J. Am. Chem. Soc.* **1965**, 87,692. Dewar, M. J. S.; De Llano, C. *J. Am. Chem. Soc.* **1969**, 91, 789; Mo, Y.; Wu, W.; Zhang, Q. *J. Chem. Phys.* **2003**, 119, 6448. Mo, Y. *J. Org. Chem.* **2004**, *69*, 5563.

**Table 4.** Weights of the VB Structures at Levels I and II Noted $w_I//w_{II}$ (lanl2dz*). The Weights of Level VB−II Are in Bold (Back-Donation On)

| VB structures | Pd−$NH_3$ | Pd−$PH_3$ | Pd−$CH_2$ | Pd−$SiH_2$ |
|---|---|---|---|---|
| 1 | 0.79//**0.78** | 0.59//**0.57** | 0.52//**0.38** | 0.44//**0.39** |
| 2 | 0.24//**0.25** | 0.48//**0.50** | 0.53//**0.67** | 0.66//**0.69** |
| 3 | −0.03//−**0.03** | −0.07//−**0.07** | −0.05//−**0.06** | −0.10//−**0.08** |

The current approach is not an optimization tool but shows an interesting trend as the metal−ligand bond distance expectedly decreases when back-donation is at work. This bond shrinking is particularly significant for second-row ligands (0.1 to 0.2 Å) and almost insignificant for the Pd−$NH_3$ complex (0.01 Å), which has the smallest back-bonding energy.

**Wave Function Analysis.** Our VB function with the lanl2dz* basis set aims at providing a simple look at the nature of the metal−ligand interaction. The VB−II wave function is a linear combination of the three VB structures, 1, 2, and 3, shown in Scheme 2. The weights[29] for these structures, as a percentage, can be used to briefly discuss the very nature of the ligand. They are displayed in Table 4 for two levels of calculation, when the back-donation is switched off ($w_I$), and when the back-donation is switched on ($w_{II}$, in bold).

In all of the cases, the weight of diionic **3** is very small and shall not be used for further analysis.[30] We shall first consider $w_{II}$ in Table 4. In the amine and phosphine ligands, neutral **1** is paramount, which illustrates the two-electron nature of such L ligands. On the contrary, and it is consistent with the usual Schrock denomination, **2** is the dominant structure for the carbene and silene complexes. It can be read formally as a covalent $\sigma$ bond supplemented with a $\pi$ bond. This is compatible with a stronger donation interaction in Pd−$XH_2$ as compared with those in Pd−$XH_3$ complexes. This last result confirms the results of Cundari and Gordon,[31] who determined the Schrock characteristics for several metal−$CH_2$ and metal−$SiH_2$ complexes.[32]

Table 4 also shows how the weights of the structures change when the back-donation in switched on or off. When the back-donation from the metal is switched on, the donation from the ligand rises up so **1** diminishes and **2** increases in weight. The modification of the weights is small for both $XH_3$ ligands, but this synergy between donation and back-donation is logically much larger for the $XH_2$ ligands.

## Conclusion

The simple and compact form of the wave function at the VB level II shows that the DCD model, as well as the VB

(29) Chirgwin, H. B.; Coulson, C. A. *Proc. R. Soc. London, Ser. A* **1950**, *2*, 196.

(30) Additionnaly, these weights are negative, which comes from the overlap terms of the Coulson−Chirgwin formula. Similar weights have already been described for minor structures, in the case of first row transition-metal-hydride cations. See Galbraith, J. M.; Shurki, A.; Shaik S. *J. Phys. Chem. A* **2000**, *104*, 1262.

(31) Cundari, T. R.; Gordon, M. S. *J. Phys. Chem.* **1992**, *96*, 631; *Organometallics* **1992**, *11*, 3122.

(32) See also the Spin Coupled Valence Bond study from Ogliaro, F.; Loades, S. S.; Cooper, D. L. *J. Phys. Chem. A* **2000**, *104*, 7091.

wave function based on it (VB-II), captures most of the chemical nature of metal−ligand bonds. From the difference between CCSD(T) and the CASSCF levels, we illustrated how important dynamical correlation is here, and we show the simplicity and the accuracy of modern BOVB type of approaches.

The comparison between VB levels I and II allows an accurate quantification of adiabatic back-bonding energies for these typical systems with contrasted behavior. Whereas the $\sigma$ bond strength is almost identical in Pd−$NH_3$ and Pd−$PH_3$ systems, back-donation appears to be almost negligible in the former complex, whereas it represents a significant part of the total bonding energy in the phosphine complex. In Pd−$CH_2$, the back-donation appears to be even the most important source of bonding, which is an unprecedented result as compared with previous studies using energy decomposition analysis. On the contrary, the $\sigma$ bond is larger than the $\pi$ bond in Pd−$SiH_2$. These trends are in line with qualitative MO analysis and are consistent with previous studies. They are also consistent with the L character of the amine ligand (as an electron pair) and rather an X type of ligand for Pd−$CH_2$ and Pd−$SiH_2$ complexes, as shown by the analysis of the VB wave function, in terms of weights. The synergy between donation and back-donation is large with these $XH_2$ ligands but very small for these $XH_3$ ligands.

**Acknowledgment.** Pr Wei Wu is most gratefully acknowledged for providing the XMVB code. M.L. is thankful to the French ministry of research (fellowship). This work was supported by substantial computing facilities from "CRIHAN, Plan Interrégional du Bassin Parisien" (project 2001-003), and the "Centre Régional de Compétence en Modélisation Moléculaire de Marseille".

**Supporting Information Available:** Coordinates and absolute energies for all of computed structures at all of the levels. This material is available free of charge via the Internet at http://pubs.acs.org.

IC701434E